

STANDARD THERMODYNAMIC PROPERTIES OF Ag_3Sn (SHOSANBETSUITE): EMF DATA

© 2025 M. V. Voronin, E. G. Osadchii*

Korzhinskii Institute of Experimental Mineralogy (IEM), Russian Academy of Sciences,

Chernogolovka, Russia

*e-mail: euo@iem.ac.ru

Received July 19, 2024

Revised August 29, 2024

Accepted September 17, 2024

Abstract. Thermodynamic properties of shosanbetsuite (Ag_3Sn) are first determined in the $\text{Ag}-\text{Sn}$ system in a galvanic cell (–) $\text{Pt} \mid \text{Gr} \mid \text{Ag} \mid \text{RbAg}_4\text{I}_5 \mid \text{Ag}_3\text{Sn}, \text{Sn} \mid \text{Gr} \mid \text{Pt}$ (+) within the temperature range of 327–427 K in vacuum. Analysis of the data makes it possible to calculate the standard (298.15 K, 10^5 Pa) $\Delta_f G^\circ$, $\Delta_f H^\circ$ and S° of Ag_3Sn : $-21238 \text{ J}\cdot\text{mol}^{-1}$, $-18763 \text{ J}\cdot\text{mol}^{-1}$ and $187.5 \text{ J}\cdot\text{K}^{-1}\cdot\text{mol}^{-1}$, respectively.

Keywords: $\text{Ag}-\text{Sn}$, Ag_3Sn , EMF-method, shosanbetsuite

DOI: 10.31857/S00167525250204e2

INTRODUCTION

Silver stannides (Ag_3Sn (ε) and Ag_4Sn (ζ)) are investigated as components of lead-free solders (Esaka et al., 2005; Kotadia et al., 2014; Cui et al., 2023; Hou et al., 2023), as well as serving as anodes for lithium-ion batteries (Wachtler et al., 2002). During the past decade, one of these intermetallic compounds (Ag_3Sn) has been found in a gold-bearing variety associated with stannides (AuSn_4 , AuSn_2 (rumoite) and AuSn (yuanjiangite)) and other gold intermetallics (Fig. 1) in placer deposits of the Olkhovaya 1st River (Kamchatsky Mys Peninsula, Eastern Kamchatka, Russia) and the Baimka River (Western Chukotka, Russia) (Sandimirova et al., 2013; Litvinenko, 2017). Subsequently, it was also discovered in the Shosanbetsu River (Haboro Town, Rumoi Province, Hokkaido Prefecture, Japan), where it was named shosanbetsuite (Nishio-Hamane, Saito, 2021). Therefore, understanding the phase relations and thermodynamic stability of phases in the $\text{Ag}-\text{Sn}$ system is essential for comprehending the processes involving these compounds, selecting optimal application conditions, and determining their formation conditions in natural environments.

In the binary system $\text{Ag}-\text{Sn}$ (Fig. 2) two intermetallic compounds are established – Ag_3Sn (ε) and Ag_4Sn (ζ) (Karakaya, Thompson, 1987). Ag_3Sn crystallizes in the orthorhombic syngony, space group $Pmmn$, cell parameters (nm): $a = 0.59682$, $b = 0.47802$, $c = 0.5184$ (Fairhurst, Cohen, 1972) and has a stoichiometric composition (Ag_3Sn) from the tin side. At a temperature of 221°C and a silver content of 3.8 at.% (Karakaya, Thompson, 1987) eutectic crystallization occurs in the system ($L = \text{Ag}_3\text{Sn} + \text{Sn}$).

There is extensive information in the literature on the investigation of thermodynamic properties in the melt region by electrochemical and calorimetric methods (Karakaya, Thompson, 1987, with cited literature), but in the solid-phase region, information is limited to determining enthalpy (Kleppa, 1955; Flandorfer et al., 2007; Ipser et al., 2007), measuring high-temperature heat capacity (Wallbrecht et al., 1981), as well as data obtained from optimization of thermodynamic properties of the $\text{Ag}-\text{Sn}$ system (Chevalier, 1988; Kattner, Boettinger, 1994; Xie, Qiao, 1996; Franke, Neuschütz, 2002). There is no information in the literature on determining the thermodynamic properties of Ag_3Sn using the EMF method.

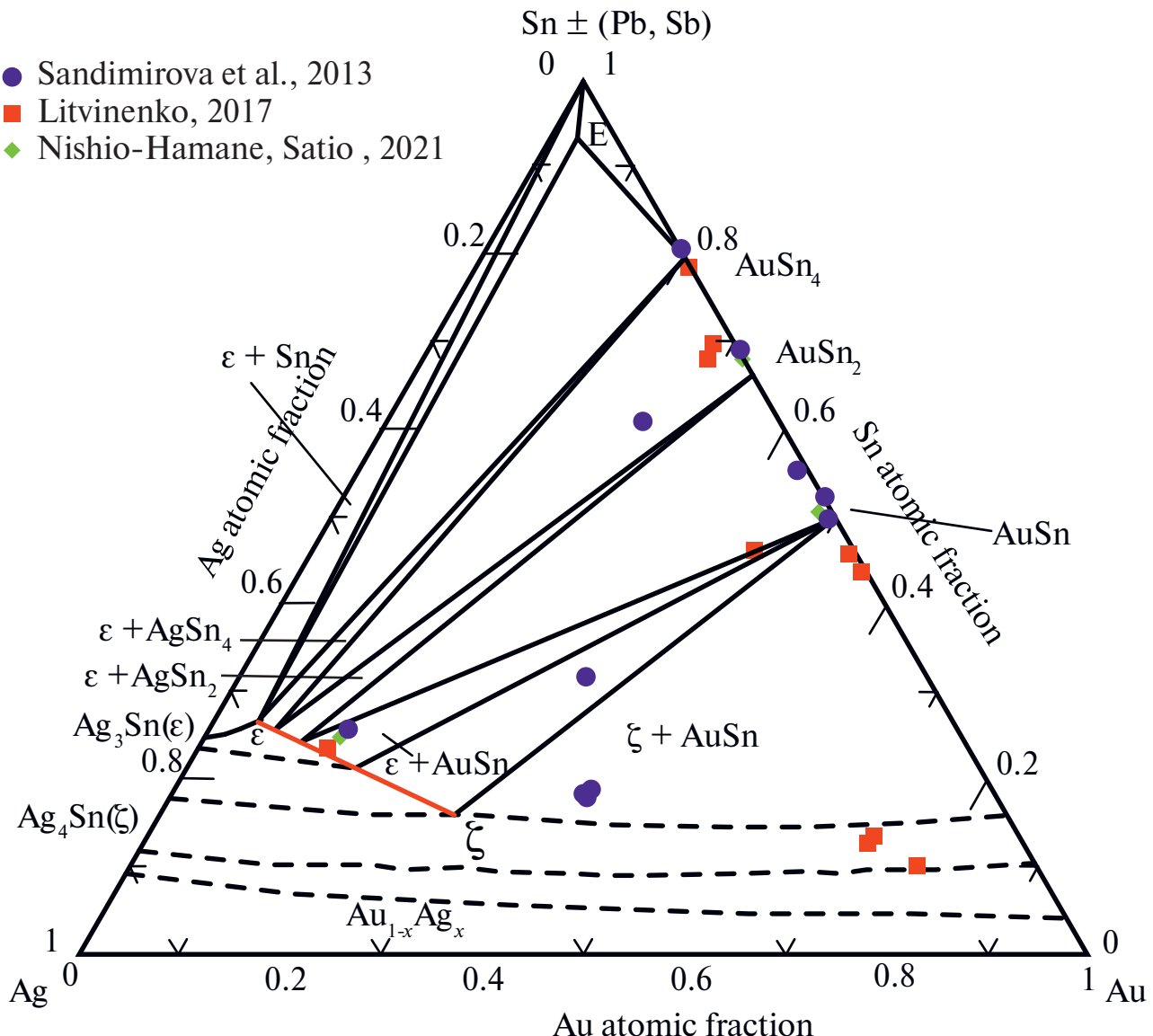


Fig. 1. Natural compositions in the Ag–Au–Sn (\pm Pb,Sb) system compared with experimental data for the Ag–Au–Sn system at 206°C (Prince et al., 2006). E – ternary eutectic

EXPERIMENTAL PART

Synthesis and characterization of solid phases. For electrochemical measurements, a mixture of $\text{Ag}_3\text{Sn} + \text{Sn}$ phases was synthesized from elements (92 at.% Sn). The synthesis was carried out by vacuum melting of a specified mixture of Ag (99.95) and Sn (99.999) metals in the amount of 3 g in a quartz glass ampoule in the flame of an oxygen burner. The sample in the form of a droplet was processed to transform it into a disk with a thickness of approximately 2 mm and a diameter of 6 mm (sample system). The X-ray diffraction pattern of the obtained sample contains two phases,

which correspond to PDF cards: 01-074-9567 for Ag_3Sn and 01-089-4898 for Sn.

Fabrication of EMF cell electrodes. The reference system (reference electrode) was made from a silver rod and was a tablet with a diameter of 6 mm and a height of 2 mm. The procedure for manufacturing the sample system is described above. Inert graphite electrodes were made from a pressed spectroscopically pure graphite rod with a diameter of 6 mm and connected to a platinum wire with a diameter of 0.2 mm. A monolithic crystalline RbAg_4I_5 was used as a solid electrolyte, manufactured at the Institute of Microelectronics Technology and High-Purity Materials of the Russian Academy of Sciences

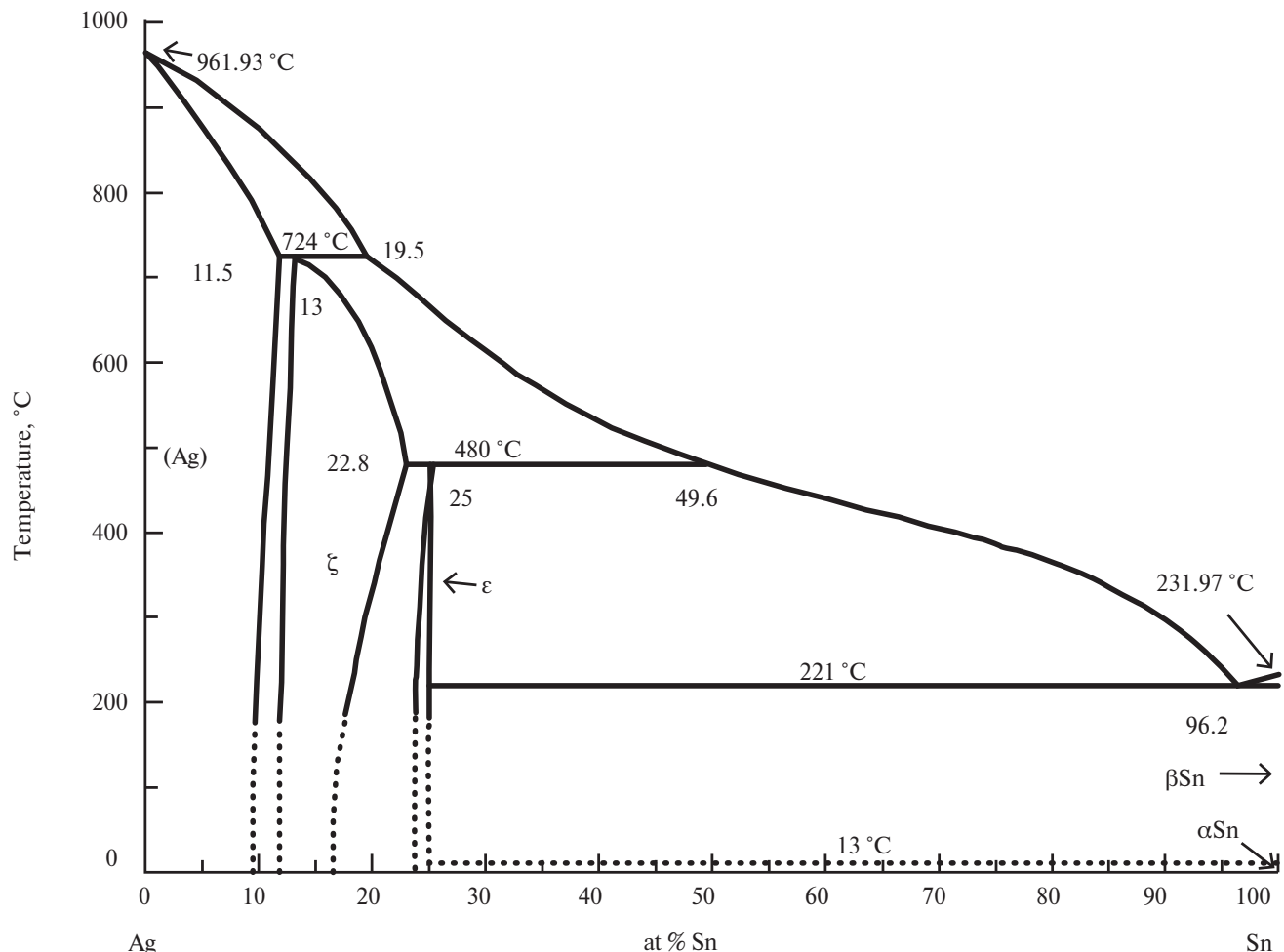


Fig. 2. Phase diagram of the Ag–Sn system according to (Karakaya, Thompson, 1987)

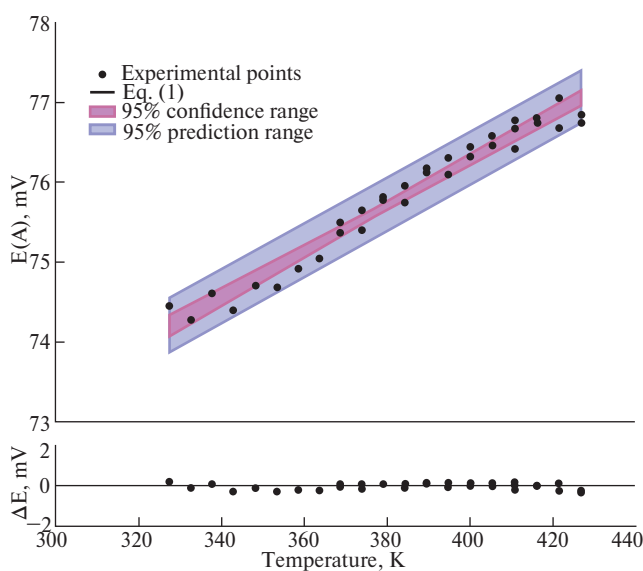


Fig. 3. Experimental values of $E(T)$ obtained in cell (A). The residual plot is shown below

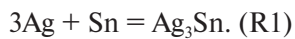
(Chernogolovka). All flat working surfaces (electrical contacts) of the electrodes were polished to a mirror shine. The schematic diagram of the electrochemical cell is presented in the work (Voronin, Osadchii, 2011).

EMF measurements. Measurements were performed using a universal multi-channel computer system (Zhdanov et al., 2005). The channels for measuring EMF have an input impedance of at least 10^{12} Ohm. Temperature was measured with a chromel-alumel thermocouple (type “K”). The accuracy of EMF and temperature measurements was ± 0.02 mV and ± 0.15 K, respectively. The experiments were conducted using the “temperature titration” method (Osadchii, Echmaeva, 2007), i.e., waiting for the establishment of a constant (equilibrium) EMF value at a given temperature. Determination of equilibrium EMF values was carried out in the mode of stepwise heating and cooling of the cell according to the procedure detailed in (Osadchii, Rappo, 2004).

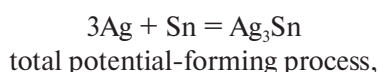
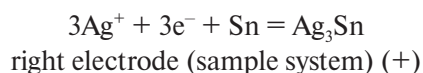
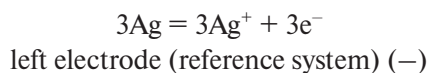
Table 1. Values of $E(T)$ measured in cell (A), ($\Delta E = E_{\text{meas.}} - E_{\text{calc.}}$)

| $T, \text{ K}$ | $E, \text{ mV}$ | ΔE | $T, \text{ K}$ | $E, \text{ mV}$ | ΔE |
|----------------|-----------------|------------|----------------|-----------------|------------|
| 410.85 | 76.42 | -0.19 | 348.15 | 74.71 | -0.10 |
| 400.18 | 76.32 | 0.01 | 337.68 | 74.61 | 0.10 |
| 389.57 | 76.13 | 0.13 | 327.41 | 74.45 | 0.23 |
| 379.08 | 75.81 | 0.11 | 332.58 | 74.28 | -0.09 |
| 368.75 | 75.50 | 0.09 | 342.80 | 74.40 | -0.26 |
| 373.85 | 75.65 | 0.10 | 353.34 | 74.69 | -0.27 |
| 384.28 | 75.96 | 0.11 | 363.68 | 75.05 | -0.21 |
| 394.79 | 76.31 | 0.16 | 373.89 | 75.41 | -0.14 |
| 405.40 | 76.58 | 0.12 | 384.20 | 75.75 | -0.10 |
| 416.22 | 76.75 | -0.02 | 394.77 | 76.10 | -0.05 |
| 426.93 | 76.84 | -0.24 | 405.47 | 76.46 | 0.00 |
| 421.53 | 76.68 | -0.24 | 416.16 | 76.80 | 0.03 |
| 410.88 | 76.67 | 0.05 | 426.83 | 76.75 | -0.32 |
| 400.14 | 76.32 | 0.01 | 421.49 | 77.05 | 0.13 |
| 389.60 | 76.17 | 0.17 | 410.83 | 76.77 | 0.16 |
| 379.14 | 75.78 | 0.08 | 400.21 | 76.45 | 0.14 |
| 368.70 | 75.37 | -0.03 | 389.53 | 76.12 | 0.12 |
| 358.54 | 74.92 | -0.19 | 379.07 | 75.81 | 0.11 |

Phase reactions and galvanic cells. In the binary Ag–Sn system, in accordance with the phase diagram (Fig. 2), the following virtual chemical reaction was studied:



For the reaction of Ag_3Sn formation from the elements, the electrochemical process is written as follows:



which coincides with reaction (R1) and is implemented in a completely solid-state galvanic cell:



where RbAg_4I_5 – Ag^+ -conducting solid electrolyte, Gr is a graphite electrode with a platinum (Pt) electrical contact.

CALCULATIONS AND RESULTS

EMF values. The results of measuring $E(T)$ dependence in cell (A) are presented in Table 1 and as a linear equation (1), provided that $\Delta_r C_p$ is constant and equal to zero (Fig. 3):

$$E(\text{A}), \text{ mV} = (64.82 \pm 0.74) + (0.02868 \pm 1.91 \cdot 10^{-3}) \cdot T, \quad (1)$$

$$(327 < T/\text{K} < 427), R^2 = 0.9638, k = 36,$$

where k is the number of experimental points, R^2 is the coefficient of determination of experimental points. According to the residual plot in Figure 3,

Table 2. Standard (298.15 K, 10⁵ Pa) thermodynamic properties of Ag₃Sn, Ag and Sn

| Phase | $\Delta_f G^\circ$ (J·mol ⁻¹) | S° (J·K ⁻¹ ·mol ⁻¹) | $\Delta_f H^\circ$ (J·mol ⁻¹) | Reference |
|-----------------------|--|--|--|---------------------------|
| Ag | 0 | 42.677 | 0 | Barin, 1995 |
| Sn | 0 | 51.195 | 0 | “” |
| Ag ₃ Sn(ε) | -18983 | 184.1 | -17528 | Chevalier, 1988 |
| | -15772 | 193.5 | -11508 | Kattner, Boettinger, 1994 |
| | -25201 | 212.1 | -15394 | Xie, Qiao, 1996 |
| | -18544 | 190.1 | -15304 | Franke, Neuschütz, 2002 |
| | - | - | -17154 ± 1673 | Glushko, 1965–1982 |
| | - | - | -16800 ± 4000* | Flandorfer et al., 2007 |
| | - | - | -16720 ± 4000** | Ipser et al., 2007 |
| | -21238 ± 51 | 187.5 ± 0.6 | -18763 ± 214 | this study |

*For composition Ag_{2.96}Sn_{1.04}. **for composition Ag_{2.976}Sn_{1.024}**Table 3.** Gibbs energy values ($\Delta_f G^\circ(T)$, J·mol⁻¹) for Ag₃Sn in the temperature range 300–500 K according to different authors

| Reference | Temperature, K | | | | |
|---------------------------|----------------|--------|--------|--------|--------|
| | 300 | 350 | 400 | 450 | 500 |
| Chevalier, 1988 | -18992 | -19236 | -19480 | -19724 | -19968 |
| Kattner, Boettinger, 1994 | -15798 | -16514 | -17229 | -17944 | -18659 |
| Xie, Qiao, 1996* | -25262 | -26906 | -28551 | -30196 | -31840 |
| Franke, Neuschütz, 2002 | -18566 | -19109 | -19653 | -20196 | -20740 |
| our data | -21253 | -21668 | -22083 | -22498 | -22913 |

*Calculated using the equation $\Delta_f G^\circ(T)$ (J·mol⁻¹) = -15394 - 32.892T

there is no reason to choose a higher-order equation to describe $E(T)$ and, accordingly, $\Delta_f G(T)$. Here and further, standard errors are given for 95% ($t_{975:36-2} = 2.032244$).

Calculation of thermodynamic values. Gibbs energy, entropy, and enthalpy of the reaction were calculated using the basic equations of thermodynamics from the temperature dependences of EMF (E , mV) of the galvanic cell:

$$\Delta_f G(J\cdot mol^{-1}) = -n\cdot F\cdot 10^{-3} E;$$

$$\Delta_f S(J\cdot K^{-1}\cdot mol^{-1}) = n\cdot F\cdot 10^{-3}\cdot (dE/dT);$$

$$\Delta_f H(J\cdot mol^{-1}) = -n\cdot F\cdot 10^{-3}\cdot [E - (dE/dT)\cdot T],$$

where $n = 3$ is the number of electrons in reaction (R1), E is the EMF in millivolts, and $F = 96485.34$ C·mol⁻¹ is the Faraday constant.

Using auxiliary data on the entropies of silver and tin, the standard thermodynamic properties of silver stannide were calculated. The obtained values, as well as auxiliary and literature data, are presented in Table 2.

The root mean square error of the regression equation $\Delta_f G^\circ(T)$ equals $\hat{\sigma} = 91$ J·mol⁻¹. The confidence interval of $\Delta_f G^\circ(T)$ at 298.15 K is 51 J·mol⁻¹. The prediction interval of $\Delta_f G^\circ(T)$ at 298.15 K equals 105 J·mol⁻¹. Thus, the confidence interval of the predicted (extrapolated) value

of $\Delta_f G^\circ$ (298.15 K) is almost twice smaller than the root mean square error of the regression equation. Electrochemical experiments are among the most accurate methods for determining the thermodynamic properties of simple compounds. Often, a greater error in calculations of complex reactions is introduced by the use of auxiliary values – thermodynamic properties of compounds participating in the studied reaction. In this work, the calculation of $\Delta_f G^\circ(T)$ for Ag_3Sn did not require using the Gibbs energy of other compounds, therefore the confidence interval of $\Delta_f G^\circ(T)$ corresponds to the confidence interval of the Gibbs energy of reaction, $\Delta_r G^\circ(T)$, obtained solely from the electrochemical experiment.

DISCUSSION

Previously, the values of thermodynamic properties for Ag_3Sn were obtained indirectly from the optimization of the Ag–Sn phase diagram, based on numerous experimental data on phase relationships in the system and thermodynamic data obtained in the melt region (Chevalier, 1988; Kattner, Boettinger, 1994; Xie, Qiao, 1996; Franke, Neuschütz, 2002). Data for Ag_3Sn in these works is typically presented as an equation of temperature dependence of Gibbs energy. It should be noted that these works do not always specify the temperature range of applicability of the equation, and do not always indicate which standard state of elements is used for the Gibbs energy data, but probably the standard state of silver and tin is crystalline at 298.15 K and 10^5 Pa. Then the specified equations can be used up to the melting temperature of tin (504 K).

Comparison of literature data with the data obtained in this work is presented in Table 3 and Figure 4. One can note a somewhat overestimated value of Gibbs energy given in (Chevalier, 1988; Kattner, Boettinger, 1994; Franke, Neuschütz, 2002) compared to the data of the present work. In (Xie, Qiao, 1996), an error was most likely made in the presented equation of temperature dependence of Gibbs energy, since in that case below 500 K the value becomes positive, and the phase becomes metastable (i.e., it is high-temperature), which contradicts the direct conclusions of both the work itself and the data of other authors. Based on the above, the sign of the constant term in the equation from the above-mentioned work was changed. Despite this, the data from (Xie, Qiao, 1996) differ significantly both from our data and from the data of other authors (Table 3, Fig. 4).

The significant discrepancies between the $\Delta_f G^\circ(T)$ values for Ag_3Sn obtained from optimization

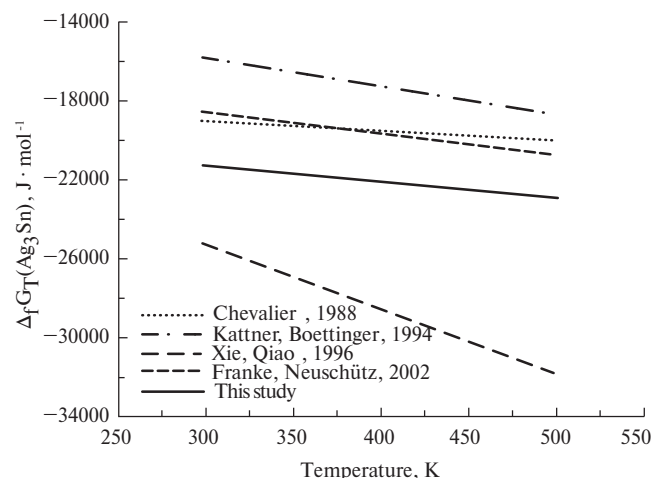


Fig. 4. Temperature dependence of Gibbs energy of Ag_3Sn according to different authors

of the Ag–Sn system and those derived from direct EMF measurements in this study indicate the need for re-optimization of the Ag–Sn system thermodynamics incorporating the newly obtained results.

The fact that shosanbetsuite has been found only in placer deposits leaves open the question regarding the formation of its associated assemblages – specifically whether it forms in primary ores and hydrothermally altered rocks or directly within the placers themselves (Sandimirova et al., 2013). Nevertheless, the new data allow evaluation of the physicochemical conditions required for shosanbetsuite formation in endogenous processes.

ACKNOWLEDGEMENTS

The authors thank the scientific editor of the article O.L. Kuskov and two anonymous reviewers for their helpful comments.

FUNDING

The work was carried out within the framework of the state assignment of the IEM RAS (FMUF-2022-0002).

REFERENCES

1. Voronin M.V., Osadchii E.G. (2011). Determination of thermodynamic properties of silver selenide by the method of galvanic cell with solid and liquid electrolytes. *Electrochemistry*. 47, 446–452.

2. Glushko V.P. (Ed.). (1965–1982). *Thermal constants of substances: Reference book in 10 issues*. Moscow: VINITI, electronic version (under the guidance of Iorish V.S. and Yungman V.S.); <https://www.chem.msu.ru/cgi-bin/tkv.pl?show=welcome.html>.
3. Zhdanov N.N., Osadchii E.G., Zotov A.V. (2005). Universal measuring system for electrochemical measurements in hydrothermal and condensed media. *Proceedings of the XV Russian Conference on Experimental Mineralogy*. Syktyvkar: “Geoprint” Publishing House, 166–168.
4. Litvinenko I.S. (2017). Gold intermetallics from the placer of the Baimka River (Western Chukotka). *Proceedings of the Russian Mineralogical Society*. 146(5), 31–43.
5. Sandimirova E.I., Sidorov E.G., Chubarov V.M., Ibragimova E.K., Antonov A.V. (2013). Native metals and intermetallics in the heavy mineral halos of the Olkhovaya 1 River (Kamchatsky Cape, Eastern Kamchatka). *Proceedings of the Russian Mineralogical Society*. 142(6), 78–88.
6. Barin I. (1995). *Thermochemical data of pure substances*. Third Edition. Two Volumes: vol. I (Ag–Kr) and vol. II (La–Zr). VCH: New York, 1900 p.
7. Chevalier P.Y. (1988). A thermodynamic evaluation of the Ag–Sn system. *Thermochim. Acta*. 136, 45–54.
8. Cui Y., Xian J.W., Zois A., Marquardt K., Yasuda H., Gourlay C.M. (2023). Nucleation and growth of Ag_3Sn in Sn–Ag and Sn–Ag–Cu solder alloys. *Acta Mater.* 249, 118831.
9. Esaka H., Shinozuka K., Tamura M. (2005). Evolution of structure unidirectionally solidified Sn– Ag_3Sn eutectic alloy. *Mater. Trans.* 46(5), 916–921.
10. Fairhurst C.W., Cohen J.B. (1972). The crystal structures of two compounds found in dental amalgam: Ag_2Hg_3 and Ag_3Sn . *Acta Crystallogr., Sect. B: Struct. Crystallogr. Cryst. Chem.* 28(2), 371–378.
11. Flandorfer H., Saeed U., Luef C., Sabbar A., Ipser H. (2007). Interfaces in lead-free solder alloys: Enthalpy of formation of binary Ag–Sn, Cu–Sn and Ni–Sn intermetallic compounds. *Thermochim. Acta*. 459(1–2), 34–39.
12. Franke P., Neuschütz D. (eds.). (2002). Ag–Sn (Silver-Tin). *Landolt-Börnstein – Group IV “Physical Chemistry”*, Volume 19 “Thermodynamic Properties of Inorganic Materials”, Subvolume 19B1 “Binary Systems. Part 1: Elements and Binary Systems from Ag–Al to Au–Tl”. Springer-Verlag Berlin Heidelberg, 4 p.
13. Hou N., Xian J.W., Sugiyama A., Yasuda H., Gourlay C.M. (2023). Ag_3Sn morphology transitions during eutectic growth in Sn–Ag alloys. *Metall. Mater. Trans. A*. 54(3), 909–927.
14. Ipser H., Flandorfer H., Luef C., Schmetterer C., Saeed U. (2007). Thermodynamics and phase diagrams of lead-free solder materials. *J. Mater. Sci.: Mater. Electron.* 18, 3–17.
15. Karakaya I., Thompson W.T. (1987). The Ag–Sn (silver-tin) system. *Bull. Alloy Phase Diagrams*. 8(4), 340–347.
16. Kattner U.R., Boettinger W.J. (1994). On the Sn–Bi–Ag ternary phase diagram. *J. Electron. Mater.* 23, 603–610.
17. Kleppa O.J. (1955). A calorimetric investigation of the system silver-tin at 450°C. *Acta Metall.* 3(3), 255–259.
18. Kotadia H.R., Howes P.D., Mannan S.H. (2014). A review: On the development of low melting temperature Pb-free solders. *Microelectron. Reliab.* 54(6–7), 1253–1273.
19. Nishio-Hamane D., Saito K. (2021). Au(Ag)–Sn–Sb–Pb minerals in association with placer gold from Rumoi province of Hokkaido, Japan: a description of two new minerals (rumoite and shosanbetsuite). *J. Mineral. Petrol. Sci.* 116(5), 263–271.
20. Osadchii E.G., Echmaeva E.A. (2007). The system Ag–Au–Se: Phase relations below 405 K and determination of standard thermodynamic properties of selenides by solid-state galvanic cell technique. *Am. Mineral.* 92, 640–647.
21. Osadchii E.G., Rappo O.A. (2004). Determination of standard thermodynamic properties of sulfides in the Ag–Au–S system by means of a solid-state galvanic cell. *Am. Mineral.* 89, 1405–1410.
22. Prince A., Liang P., Tedenac J.-C., Lakiza S., Dobatkina T. (2006). Ag–Au–Sn (Silver-Gold-Tin). *Landolt-Börnstein – Group IV “Physical Chemistry”*, Volume 11 “Ternary Alloy Systems – Phase Diagrams, Crystallographic and Thermodynamic Data critically evaluated by MSIT”, Subvolume 11B “Noble Metal Systems. Selected Systems from Ag–Al–Zn to Rh–Ru–Sc”. Effenberg G., Ilyenko S. (eds.), Springer-Verlag Berlin Heidelberg, 11 p.
23. Wachtler M., Winter M., Besenhard J.O. (2002). Anodic materials for rechargeable Li-batteries. *J. Power Sources*. 105, 151–160.
24. Wallbrecht P.C., Blachnik R., Mills K.C. (1981). The heat capacity and enthalpy of some Hume-Rothery phases formed by copper, silver and gold. Part II. Cu+Ge, Cu+Sn, Ag+Sn, Au+Sn, Au+Pb systems. *Thermochim. Acta*. 46(2), 167–174.
25. Xie Y., Qiao Z. (1996). Thermodynamic reoptimization of the Ag–Sn system. *J. Phase Equilib.* 17, 208–217.